INTELLIGENCE Journal of Multidisciplinary Research
(A Peer Reviewed, Open Access International Journal)
ISSN 2822-1869 (Print); ISSN 2822-1877 (Online)
Volume 4, Issue 1, March 2025, pp 67-80
Research Management Cell, Pokhara Multiple Campus, Pokhara, Nepal
Email: research.intelligencepmcrmc021@gmail.com URL: www.pmcpokhara.edu.np
DOI: https://doi.org/10.3126/ijmr.v4i1.76932

Article History
Received: 18 December 2024
Revised: 14 February 2025
Accepted: 27 February 2025

Synthesis, Characterization, and Structural Elucidation of a Novel (E)-1-(1-Phenyl-1H-pyrazol-4-yl) -N-(1-(p-tolyl)-1H-pyrazol-5-yl)methanimine

[1] Kamal Raj Sapkota

Abstract

(E)-1-(1-Phenyl-1H-pyrazol-4-yl)-N-(1-(p-tolyl)-1H-pyrazol-5-yl)methanimine (PPM) was synthesized by reacting 1-phenyl-1H-pyrazole-4-carbaldehyde with 1-(p-tolyl)-1H-pyrazol-5-amine in methanol, achieving a 90% yield. The elemental analysis confirmed the molecular formula, $C_{17}H_{13}N_5$. Structural characterization was performed using NMR, IR, UV-Vis spectroscopy, and mass spectrometry. The 1H and 13C NMR spectra identified the imine, aromatic, and pyrazole groups, verifying the molecular structure. IR analysis showed characteristic bands for C=N, aromatic C=C, NH, and CH_3 groups, consistent with the compound's functional groups. UV-Vis spectroscopy revealed transitions at 415 nm and 325 nm, indicating an extended conjugated system. Mass spectrometry established the molecular ion at m/z 328 ([M+H]+) and identified fragmentation patterns consistent with the proposed structure. This comprehensive analysis demonstrates the successful synthesis and structural elucidation of PPM.

Keywords

Fragmentation
Methanimine
Methanol
Pyrazole

(E)-1-(1H-pyrazol-4-yl-1-phenyl) The compound -N-(1-(p-tolyl)-1H-pyrazol-5-yl)A Schiff base, methanimine (PPM) is generated from pyrazole, a class of heterocyclic chemicals that may find use in a number of disciplines, including material science, pharmaceutical chemistry, and coordination chemistry (Hassani et al., 2023; Moussa et al., 2024: Verma et al., 2023). Schiff bases have special electronic and structural characteristics due to the presence of an azomethine (-CH=N-) group (Katariya et al., 2022; Moussa et al., 2024). Due to their substantial pharmacological actions, such as antibacterial, anti-inflammatory, and anticancer qualities, pyrazole

[1] Department of Chemistry, Prithvi Narayan Campus, Tribhuvan University, Pokhara, Nepal. Email: sapkotakamal69@gmail.com

derivatives in particular have been the subject of much research (Karrouchi et al., 2018; Hassani et al., 2023; Moussa et al., 2024: Verma et al., 2023). Additionally, these substances are crucial ligands in the creation of coordination complexes, which are frequently used in sensing and catalysis applications. The five-membered heterocyclic chemical class known as pyrazoles is very important in organic synthesis. They have attracted a lot of attention because they are one of the azole family's most researched groupings. Over time, a variety of synthetic techniques and structural changes have been implemented. As a crucial component of a wide range of compounds, the pyrazole nucleus supports its numerous applications in a variety of fields, such as technology, medicine, and agriculture. This adaptability is particularly noticeable in the bioactive characteristics of derivatives of pyrazoles. They exhibit a wide range of therapeutic effects and are recognized for their potential as effective inhibitors of protein glycation. Pyrazoles are essential in the creation of innovative medical therapies and solutions because of their antibacterial, antifungal, anticancer, antidepressant, anti-inflammatory, anti-tuberculosis, antioxidant, and antiviral properties.

(E)-1-(1-phenyl-1H-pyrazol-4-yl)-N-(1-(p-tolyl)-1H-pyrazol-5-yl)methanimine (PPM) is conjugated with two pyrazole units, a phenyl group, and a p-tolyl substituent. Its chemical reactivity and possible biological activity are anticipated to be influenced by the improved conjugation and electronic interactions that such a structure offers (Silva et al., 2018; Ebenezer et al., 2022; Golovanov et al., 2021). Because they may form stable metal complexes, Schiff bases with this kind of structural complexity are frequently investigated as potential candidates for material and catalytic applications (Liu et al., 2018; Zhang et al., 2018; Cozzi, 2004). Furthermore, the electron-donating and withdrawing properties of the phenyl and p-tolyl groups may further boost its potential adaptability in numerous scientific disciplines (Raicopol et al., 2012; Wang et al., 2016; Khan et al., 2014).

To comprehend PPM's chemical and physical characteristics, its synthesis and characterisation are essential. To identify functional groups and guarantee the accuracy of the molecular structure, advanced characterisation techniques have been used. The molecular weight and fragmentation pattern are specified by mass spectrometry (MS), which also provides proof of the molecular formula. The purity of the produced product is guaranteed by elemental analysis (CHN), which verifies the proportion composition of carbon, hydrogen, and nitrogen. Characteristic functional groups, such as the azomethine (vC=N) stretching vibration at 1600 cm^{-1} (Pavia et al., 2015; Socrates, 2004), as well as vibrations belonging to aromatic and aliphatic functional groups, can be identified with the aid of infrared spectroscopy (IR).

The molecule's electronic transitions are investigated using ultraviolet-visible spectroscopy, or UV-Vis. π-π* and n-π* transitions are indicated by absorption maxima (λmax), which reveal information on the electronic characteristics of the conjugated system (Pavia et al., 2015; Pretsch et al., 2013). ^{1}H and ^{13}C nuclear magnetic resonance (NMR) spectroscopy provides comprehensive details about the chemical surroundings of carbon and hydrogen atoms. The presence of aromatic carbons and the azomethine carbon is confirmed by the ^{13}C NMR spectrum, although the ^{1}H NMR spectrum shows different signals for aromatic and azomethine protons.

These thorough analyses demonstrate the purity and structural integrity of (E)-1-(1-phe-

nyl-1H-pyrazol-4-yl)-N-(1-(p-tolyl)-1H-pyrazol-5-yl)methanimine, providing a strong basis for further research focused at examining its possible uses in a range of scientific domains. In addition to guaranteeing accurate characterisation, the combination of cutting-edge methodologies emphasizes the compound's suitability for additional material science and biological applications.

Methodology

Methods

A Perkin-Elmer FT-IR spectrometer was used to record the FT-IR spectrum of (E)-1-(1-phenyl-1H-pyrazol-4-yl)-N-(1-(p-tolyl)-1H-pyrazol-5-yl)methanimine (PPM) at 25 °C. This allowed for the identification of the molecule's vibrational modes and functional groups. A Bruker AVANCE-III spectrometer was used to perform 13C and 1H NMR spectroscopy in order to examine the structural features of the hydrogen and carbon atoms. Using a Perkin-Elmer Lambda 35 spectrometer, UV-Vis spectroscopy revealed details on the compound's electronic absorption characteristics over a wavelength range of 200 to 600 nm with a bandwidth of 1 nm. In order to ascertain the molecular ion and fragmentation pattern, the mass spectrometric analysis was conducted on a WATERS Q-ToF Premier Mass Spectrometer employing electrospray ionization (ESI-MS). Additionally, a Perkin-Elmer 2400 Series II CHNS/O Analyzer was used to evaluate the compound's elemental composition and ensure that it agreed with theoretical values.

Materials

Sigma-Aldrich provided all of the ingredients needed to synthesize (E)-1-(1-phenyl-1H-pyrazol-4-yl)-N-(1-(p-tolyl)-1H-pyrazol-5-yl)methanimine (PPM), which were employed straight into the process without any additional purification.

Results and Discussion

Synthesis of (E)-1-(1-phenyl-1H-pyrazol-4-yl)-N-(1-(p-tolyl)-1H-pyrazol-5-yl)methanimine (PPM)

PPM was synthesized by reacting 1-phenyl-1H-pyrazole-4-carbaldehyde (1) with 1-(p-tolyl)-1H-pyrazol-5-amine (2), as shown in Scheme 1. First, 0.50 g (2.88 mmol) of 1-(p-tolyl)-1H-pyrazol-5-amine was dissolved in 20 mL of methanol. Then, 0.49 g (2.84 mmol) of 1-phenyl-1H-pyrazole-4-carbaldehyde was added to the solution. The reaction mixture has been refluxed for 7 hours, during which a light yellow solid precipitate formed, and the solution volume was reduced to 10 mL. The precipitate was filtered out and washed with 5 mL cold methanol and 10 mL hexane. The resulting red powder was recrystallized from methanol and thoroughly dried in a vacuum desiccator. With a 90% yield, 0.90 g of yellow solid was the end product, PPM. The aforementioned synthetic technique has previously been documented (Jamal et al., 2024; 2025).

The molecular formula of the compound (PPM) was found to be $C_{17}H_{13}N_5$. The calculated values of C, 73.37%; H, 5.23%; and N, 21.39%, as determined by elemental analysis, closely matched the values obtained experimentally, which were C, 73.14%; H, 5.09%; and N, 21.11%. These findings provide highly accurate confirmation of the compound's elemental composition.

Additionally, Figure 1 illustrates the PPM structure.

Figure 1

Structure of PPM

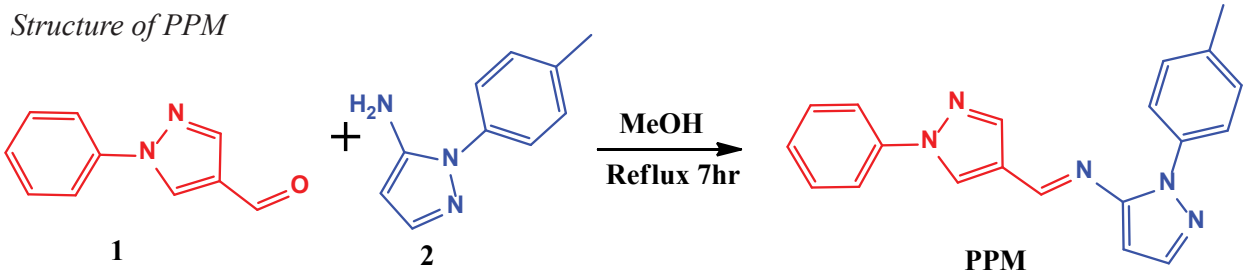

Scheme1

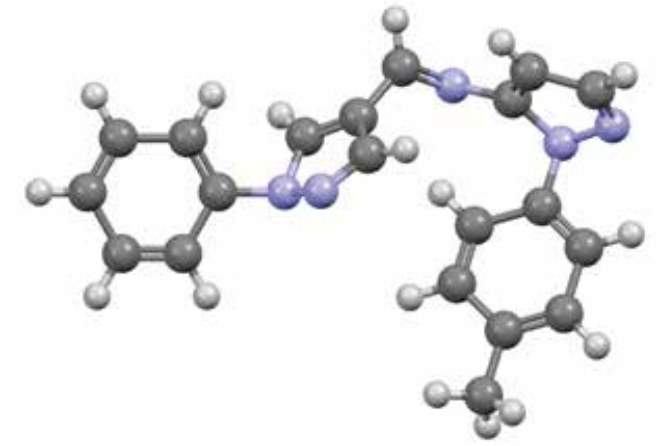

NMR study

When (E)-1-(1-phenyl-1H-pyrazol-4-yl)-N-(1-(p-tolyl)-1H-pyrazol-5-yl)methanimine was recorded in DMSO-d_6, its 1H NMR spectrum (Figure 1.1) revealed a mix of broad and sharp signals that were in line with the predicted proton environments. The presence of the C=N bond was confirmed by assigning a singlet to the imine proton at δ 8.85 ppm. At δ 7.55–7.40 ppm, the phenyl group's aromatic protons appeared as a multiplet. This finding is in line with other research on Schiff bases and compounds containing imines, which found that the deshielding effect of the nearby nitrogen typically triggers the imine proton to emerge in the downfield region (Pretsch et al., 2013; Kaya et al., 2011: Jamal et al., 2025). Similar chemical changes for imine functionalities have been documented in a number of studies, supporting the structural characterisation of these molecules.

(Pretsch et al., 2013: Meyer et al., 2007; Pavia et al., 2015) The aromatic protons in the p-tolyl group showed a doublet at δ 7.38 ppm (J = 8.1 Hz), while the methyl group showed a singlet at δ 2.34 ppm (Pavia et al., 2015; Pretsch et al., 2013). The pyrazole ring protons were represented by the broad signals in the spectrum. The pyrazole ring's NH proton was identified as the source of a wide singlet at δ 10.12 ppm, indicating that it is exchangeable. Two more broad singlets, which correspond to aromatic CH protons inside the pyrazole rings, were detected at δ 8.43 and δ 8.15 ppm (Sharma, 2007; Pavia et al., 2015; Pretsch et al., 2013). The pres-

ence of its essential functional groups is highlighted by this 1H NMR investigation, which also validates the structural integrity of (E)-1-(1-phenyl-1H-pyrazol-4-yl)-N-(1-(p-tolyl)-1H-pyrazol-5-yl)methanimine. The suggested molecular structure (PPM) is in agreement with the distribution of chemical shifts.

(E)-1-(1-phenyl-1H-pyrazol-4-yl)-N-(1-(p-tolyl)-1H-pyrazol-5-yl)methanimine's 13C NMR spectrum (Figure 1.1), which was recorded in DMSO-d_6, showed multiple unique peaks that represented the various carbon environments inside the molecule. The imine carbon (C=N), which is typical of the compound's C=N group, was identified as the source of the peak at δ 146.0 ppm (Sharma, 2007; Pavia et al., 2015; Pretsch et al., 2013). Because of conjugation and electrical effects, imimine carbons usually occur in the 140–160 ppm range (Silverstein et al., 2014; Pretsch et al., 2013). Similar shifts around δ 145–155 ppm are reported in studies on pyrazole derivatives (Silverstein et al., 2014; Sharma, 2007; Pavia et al., 2015; Pretsch et al., 2013), which validate the compound's structural integrity and corroborate our assignment. Individual aromatic carbons in the benzene ring were represented by signals at δ 128.2 ppm and δ 130.0 ppm, whereas the aromatic carbons from the phenyl group were detected in the range of δ 125.4–130.0 ppm. The carbons in the pyrazole ring provided many signals. At δ 142 ppm, the pyrazole ring's imine carbon (C=N) was visible, which is in line with the carbon that is directly bonded to the nitrogen in the heterocyclic ring. The region of δ 120.0–140.0 ppm was found to contain the aromatic carbons of the pyrazole rings (Pavia et al., 2015; Pretsch et al., 2013). These chemical shift values align with previously reported NMR studies on pyrazole derivatives, where imine carbons typically resonate between δ 140–150 ppm due to their electron-deficient nature and conjugation effects (Silverstein et al., 2014; Pavia et al., 2015; Pretsch et al., 2013). Similarly, aromatic carbons in heterocyclic systems are commonly found in the range of δ 115–145 ppm, depending on substitution patterns and electronic interactions (Sharma, 2007; Silverstein et al., 2014). The observed shifts are characteristic of pyrazole-containing compounds and further confirm the structural integrity of the synthesized molecule (Nakamoto, 2009)

At δ 138.3 and δ 130.1 ppm, the pyrazole ring displayed distinctive carbon signals that corresponded to carbons situated next to the nitrogen atom in the heterocyclic ring. The carbon at position 1 of the pyrazole ring, next to the imine group, was identified as the source of the signal at δ 121.6 ppm. A methyl group connected to an aromatic ring is consistent with the methyl carbon signal that the p-tolyl group contributed at δ 21.3 ppm. In the δ 128.0–130.0 ppm region, additional aromatic carbon signals from the p-tolyl group were detected (Sharma, 2007; Pavia et al., 2015; Pretsch et al., 2013). All things considered, the carbon habitats in (E)-1-(1-phenyl-1H-pyrazol-4-yl)-N-(1-(p-tolyl)-1H-pyrazol-5-yl)methanimine are thoroughly and consistently analyzed by the 13C NMR spectra. The presence of the phenyl, pyrazole, and p-tolyl groups as well as the imine functionality are confirmed by the peak assignments, which are in good agreement with the predicted structure.

IR study

(E)-1-(1-phenyl-1H-pyrazol-4-yl)-N-(1-(p-tolyl)-1H-pyrazol-5-yl)methanimine's infrared (IR) spectra, which was recorded between 4000 and 450 cm^{-1}, showed a number of charac

Figure 1.1

1H and 13C NMR of PPM

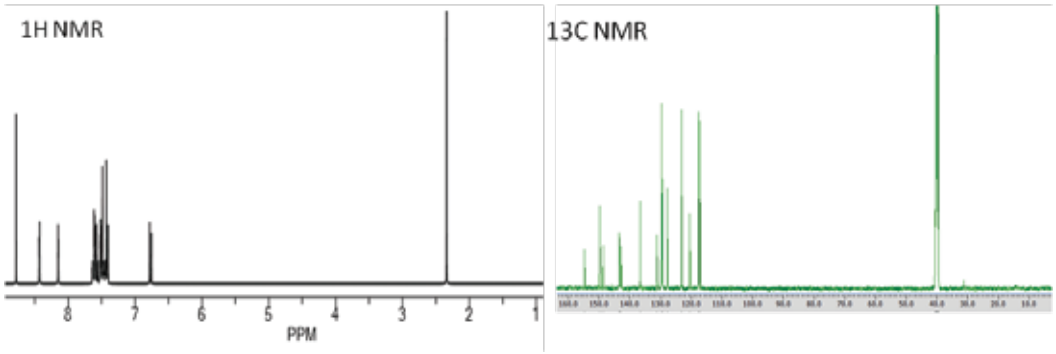

teristic absorption bands that were suggestive of the molecule's functional groups and general structure. The imine (C=N) bond's stretching vibration was identified by a strong, crisp band at 1620 cm^{-1} (Sharma, 2007; Pavia et al., 2015; Socrates, 2004). This discovery is in line with observations in the literature, which state that the distinctive C=N bond causes imine stretching vibrations to generally occur in the 1600–1650 cm^{-1} range (Silverstein et al., 2014; Pretsch et al., 2013; Socrates, 2004). Similar absorption bands have been seen in this location in studies on Schiff bases and pyrazole derivatives, indicating that the imine functionality is present (Sharma, 2007; Pavia et al., 2015).

The presence of the C=N linkage in the chemical is confirmed by this absorption, which is typical of compounds with an imine group. According to the chemical structure, the band at 1620 cm^{-1} supports the synthesis of the imine group in the molecule, and the stretching frequency for C=N bonds is normally between 1600 and 1690 cm^{-1} (Pavia et al., 2015; Socrates, 2004). The aromatic rings' C=C stretching vibrations are responsible for the notable absorption band that was detected at 1602 cm^{-1} (Socrates, 2004). The phenyl and pyrazole rings' conjugated system gives rise to this band, suggesting that these aromatic components support the structure's overall conjugation. As is common for compounds with conjugated systems, the downshifted absorption of the C=C stretch is probably caused by the conjugation in the aromatic rings. The spectrum showed distinctive C-H stretching vibrations for the aromatic protons in the 3050–3000 cm^{-1} range, which are suggestive of the hydrogen atoms joined to carbon atoms in the aromatic rings (Pavia et al., 2015; Socrates, 2004). The presence of both the pyrazole and phenyl rings in the structure is supported by these absorptions. The stretching vibrational band of the C-H bonds in the benzene ring is the cause of the bands in this area, which are common for aromatic compounds.

As is common for compounds with NH groups, particularly in heterocyclic structures like pyrazoles, the NH stretching vibration was detected as a broad, weak band at 3230 cm^{-1} (Pavia et al., 2015; Socrates, 2004). This band's broadness indicates the existence of intermolecular interactions or hydrogen bonds with the solvent or other functional groups inside the mole-

cule. This discovery is consistent with earlier observations in the literature, which state that hydrogen bonding effects are responsible for the broadening of NH stretching vibrations in pyrazole and related heterocyclic compounds, which usually occur in the region of 3200–3400 cm^{-1} (Silverstein et al., 2014; Pretsch et al., 2013). Similar patterns have been seen in studies on Schiff bases and other nitrogen-containing heterocycles, supporting the idea that hydrogen bonds affect vibrational properties (Sharma, 2007; Nakamoto, 2009). According to numerous reports in vibrational spectroscopy research, the presence of hydrogen bonding can cause peak broadening and spectrum changes (Socrates, 2004). These results support the current study's assignment of the NH stretching band.

Because the NH proton is exchangeable, the NH stretching band in pyrazole derivatives is frequently widened by the creation of hydrogen bonds.
The stretching vibrational band of the C-H bond in the methyl group (CH_3) connected to the p-tolyl group is responsible for another noticeable absorption that was seen at 2925 cm^{-1} (Socrates, 2004). The existence of the methyl group in the structure is confirmed by this absorption, which is frequently seen in compounds with methyl substituents on aromatic rings. This result is in line with findings in the literature, which state that, depending on the molecular environment, the C-H stretching vibrations of methyl groups usually occur in the range of 2850 to 2950 cm^{-1} (Silverstein et al., 2014; Pavia et al., 2015). The attribution of this absorption band has been supported by studies on methyl-substituted aromatic compounds, which have shown comparable spectrum features (Sharma, 2007; Pretsch et al., 2013). This peak's existence further bolsters the structural soundness of

Other features were seen in the fingerprint region (below 1500 cm^{-1}). The presence of the pyrazole nitrogen attached to the aromatic ring is further supported by the observation of two absorptions: one at 1365 cm^{-1}, which corresponds to the C-H bending vibrations of the aromatic rings, and another at 1200 cm^{-1}, which is generally attributed to the C-N stretching vibrations in aromatic amines (Sharma, 2007; Socrates, 2004). These assignments are consistent with earlier observations in the literature, which show that C-H bending vibrations in aromatic systems often occur between 1300 and 1400 cm^{-1} and are impacted by conjugation effects and ring substitution (Sharma, 2007; Socrates, 2004; Silverstein et al., 2014; Pavia et al., 2015). According to several spectroscopic investigations, C-N stretching vibrations in aromatic amines are frequently seen between 1180 and 1250 cm^{-1} (Pretsch et al., 2013; Nakamoto, 2009). The spectrum assignments in the current work are further supported by the numerous reports of these bands' existence in heterocyclic compounds, especially pyrazole derivatives (Sharshira et al., 2012; Silverstein et al., 2014; Pavia et al., 2015).

Additionally, the monosubstituted aromatic ring structure in the phenyl and p-tolyl groups is characterized by C-H out-of-plane bending vibrations, which are responsible for a number of weaker absorptions in the 700–800 cm^{-1} area. These bending modes, which are usually seen in the fingerprint region, offer more proof that the molecule is aromatic (Sharma, 2007; Pavia et al., 2015; Socrates, 2004).

The IR spectrum (Figure 2) of (E)-1-(1-phenyl-1H-pyrazol-4-yl)-N-(1-(p-tolyl)-1H-pyrazol-5-yl)methanimine shows absorption patterns that are consistent with the presence of methyl substituents, aromatic rings, NH groups, and imine groups. The distinctive absorption bands

show the functional groups involved and lend support to the suggested molecular structure. The thorough IR spectrum analysis validated the target molecule's effective synthesis and offered a useful insight of the compound's molecular shape.

Figure 2

IR

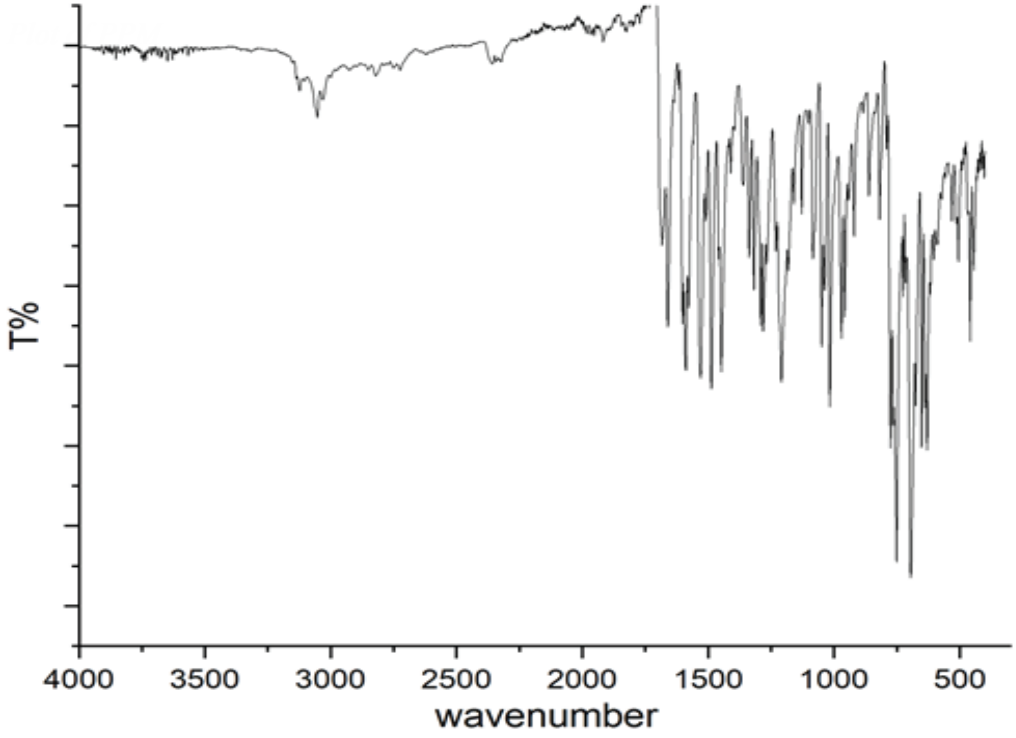

UV-Vis

Two noticeable absorption bands are visible in the UV-Vis spectrum (Figure 3) of (E)-1-(1-phenyl-1H-pyrazol-4-yl)-N-(1-(p-tolyl)-1H-pyrazol-5-yl)methanimine. These bands are suggestive of different electronic transitions that emphasize the compound's distinct electronic structure and conjugation. The sharp peak at 415 nm, which is indicative of a charge-transfer transition, is the first noteworthy feature (Sharma, 2007; Pavia et al., 2015; Pretsch et al., 2013). This peak indicates that the molecule experiences strong electrical interactions that are made possible by the imine group and the conjugation of the phenyl and pyrazole rings. By raising the electron density in the conjugated system, the p-tolyl substituent—which has an electron-donating methyl group—further improves the charge-transfer transition (Sharma, 2007; Pretsch et al., 2013). A greater overlap of electron densities between the donor and acceptor moieties is encouraged by the electron-donating development of the methyl group, which facilitates the transfer of charge (Sharma, 2007; Pavia et al., 2015). This transition, which is usually connected to π-π* or n-π* transitions, is thus seen in the lower-energy part of the spectrum. These transitions contribute to the overall electrical characteristics of the molecule by mediating the broad delocalization of π-electrons across the molecular framework (Pavia et al., 2015; Pretsch et al.,

2013). The molecule's strong charge-transfer interactions, which are frequently desired in materials meant for applications in fields including optoelectronics, organic photovoltaics, and photonic materials, are highlighted by the observed intense absorption at 415 nm. Its electrical features are facilitated by the charge-transfer transition's well-defined conjugated structure, which allows the electron density to move across the molecule effectively. A second absorption band, which corresponds to a π-π* transition mainly involving the aromatic and heteroaromatic rings, is seen at 325 nm in addition to the strong peak at 415 nm. While π-electrons are delocalized across the aromatic systems, this transition is localized within the phenyl and pyrazole rings. The π-π* transition is facilitated by the intrinsic electronic structure of these aromatic rings, as indicated by the moderate energy required for this transformation. The confined π-electron transitions, which are distinct from the charge-transfer transitions involving more extensive delocalization, are described by this band at 325 nm. The distinct electronic environments within the molecule are highlighted by the difference in the absorption wavelengths, which are 415 nm for the charge-transfer transition and 325 nm for the π-π* transition. While the absorption at 325 nm indicates the localized electronic transitions inside the aromatic rings, the strong interaction between the donor and acceptor moiety in the conjugated system is reflected by the high absorption at 415 nm (Sharma, 2007; Pavia et al., 2015; Pretsch et al., 2013). These findings show that the molecule's electrical transition behavior, electron density distribution, and conjugation all interact intricately. When combined, these spectrum features show the compound's distinct conjugated structure, which facilitates effective electronic transitions. The compound's electronic properties may be better understood thanks to the UV-Vis spectral features, which also point to the possibility of using it in applications that demand powerful charge-transfer capabilities. The observed UV-Vis behavior, which highlights the molecule's distinct electronic architecture and its promise for advanced materials applications in domains like photonics and organic electronics, is mostly determined by the interaction of aromaticity, conjugation, and the influence of substituent groups.

Figure 3

UV-Vis Plot of PPM

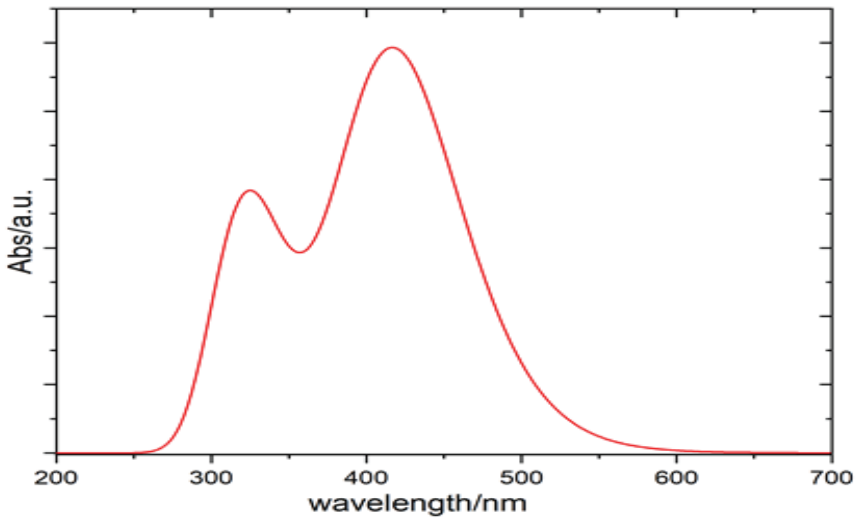

Mass Spectrometry (MS) Analysis

Using electrospray ionization (ESI) in positive ion mode, the mass spectrum of (E)-1-(1-phenyl-1H-pyrazol-4-yl)-N-(1-(p-tolyl)-1H-pyrazol-5-yl)methanimine was acquired. The molecular ion [M+H]+ was represented by a strong molecular ion peak in the spectra at m/z 328. The compound's molecular weight of 327 g/mol was verified by the high-resolution measurement, which was in line with the predicted value. The molecular ion's fragmentation produced a number of notable peaks, the base peak of which was seen at m/z 237 and indicated the removal of a p-tolyl group. At m/z 171, another important fragment ion was detected, which was explained by the pyrazole ring cleaving and losing a phenyl group. Other prominent fragment peaks were m/z 204 and m/z 176, which were compatible with normal pyrazole and imine fragmentations and were caused by subsequent rearrangements and losses of smaller neutral molecules. The mass spectrum confirmed the integrity of the produced molecule (PPM) and supported the molecular formula by offering additional proof of the compound's structure.

Conclusion

(E)-1-(1-phenyl-1H-pyrazol-4-yl)-N-(1-(p-tolyl)-1H-pyrazol-5-yl)methanimine (PPM) was successfully synthesized with a high yield of 90%, as evidenced by elemental analysis and its chemical formula $C_{17}H_{13}N_5$. The structure and characteristics of the chemical were confirmed by thorough characterization utilizing cutting-edge spectroscopic techniques. Chemical changes in the NMR measurements perfectly matched the suggested molecular structure, highlighting the presence of aromatic moieties and imine functionality. The methyl group, aromatic rings, and imine (C=N) bond were all confirmed by distinctive absorption bands in the infrared spectrum. The extended conjugated system was highlighted by the UV-Vis spectrum's $\pi \rightarrow \pi^*$ transitions (strong), and the structural integrity was supported by mass spectrometry's validation of the molecular weight and fragmentation pattern. Together, the data highlight PPM's effective synthesis and comprehensive structural elucidation, laying the groundwork for future research into its possible uses.

References

Ansari, A., Ali, A., & Asif, M. (2017). Biologically active pyrazole derivatives. *New Journal of Chemistry, 41*(1), 16–41

Cozzi, P. G. (2004). Metal–Salen Schiff base complexes in catalysis: Practical aspects. *Chemical Society Reviews, 33*(7), 410–421.

Ebenezer, O., Shapi, M., & Tuszynski, J. A. (2022). A review of the recent development in the synthesis and biological evaluations of pyrazole derivatives. *Biomedicines, 10*(5), 1124.

Fustero, S., Sánchez-Roselló, M., Barrio, P., & Simón-Fuentes, A. (2011). From 2000 to mid-2010: A fruitful decade for the synthesis of pyrazoles. *Chemical Reviews, 111*(11), 6984–7034.

G. Socrates. 2004. *Group frequencies for Raman and infrared characteristics: Tables and graphics.* Wiley & Sons, John.

Golovanov, A. A., Odin, I. S., Gusev, D. M., Vologzhanina, A. V., Sosnin, I. M., & Grabovskiy, S. A. (2021). Reactivity of cross-conjugated enynones in cyclocondensations with hydrazines: Synthesis of pyrazoles and pyrazolines. *The Journal of Organic Chemistry, 86*(10), 7229–7241.

Jamal, A., Faizi, M. S. H., & Ferjani, H. (2025). Designing of quinoline-based esterase inhibitor: Synthesis, crystal structure, DFT calculations, and molecular docking. *Journal of Molecular Structure, 1319*, 139540.

Jamal, A., Faizi, M. S. H., & Necmi, D. E. G. E. (2024). Synthesis, structural characterization, DFT calculations, and molecular docking of a novel quinoline derivative. *Journal of Molecular Structure, 1300,* 137251.

Karrouchi, K., Radi, S., Ramli, Y., Taoufik, J., Mabkhot, Y. N., Al-Aizari, F. A., & Ansar, M. H. (2018). Synthesis and pharmacological activities of pyrazole derivatives: A review. *Molecules, 23*(1), 134.

Katariya, K. D., Nakum, K. J., & Hagar, M. (2022). New fluorinated azo/schiff base liquid crystals: synthesis, characterisation, mesomorphic study and DFT calculations. *Liquid Crystals, 49*(3), 312–326.

Kaya, İ., & Uysal, S. (2011). Synthesis and characterization of imine polymers containing aliphatic and aromatic groups and some of Schiff base-metal complexes. *Journal of Applied Polymer Science, 120*(6), 3325-3336.

Khan, I., Ibrar, A., Abbas, N., & Saeed, A. (2014). Recent advances in the structural library of functionalized quinazoline and quinazolinone scaffolds: Synthetic approaches and multifarious applications. *European Journal of Medicinal Chemistry, 76*, 193–244.

Liu, X., Manzur, C., Novoa, N., Celedón, S., Carrillo, D., & Hamon, J. R. (2018). Multidentate unsymmetrically-substituted Schiff bases and their metal complexes: Synthesis, functional materials properties, and applications to catalysis. *Coordination Chemistry Reviews, 357*, 144–172.

Meyer, C. D., Joiner, C. S., & Stoddart, J. F. (2007). Template-directed synthesis employing reversible imine bond formation. *Chemical Society Reviews, 36*(11), 1705-1723.

Moussa, Z., Ramanathan, M., Alharmoozi, S. M., Alkaabi, S. A. S., Al Aryani, S. H. M., Ahmed, S. A., & Al-Masri, H. T. (2024). Recent highlights in the synthesis and biological significance of pyrazole derivatives. *Heliyon*.

Nakamoto, K. (2009). *Infrared and Raman spectra of inorganic and coordination compounds, Part A: Theory and applications in inorganic chemistry* (6th ed.). Wiley.

Pavia, D. L., Lampman, G. M., Kriz, G. S., & Vyvyan, J. R. (2015). *Introduction to spectroscopy*.

Pretsch, E., Clerc, T., Seibl, J., & Simon, W. (2013). *Tables of spectral data for structure determination of organic compounds*. Springer Science & Business Media. Raicopol, M., Necula, L., Ionita, M., & Pilan, L. (2012). Electrochemical reduction of aryl diazonium salts: a versatile way for carbon nanotubes functionalisation. *Surface and Interface Analysis, 44*(8), 1081–1085.

Rouzi, K., Assila, H., Karrouchi, K., Ameziane El Hassani, I., & Ansar, M. H. (2023). A summary of recent developments in the synthesis of pyrazole derivatives. *Reactions, 4*(3), 478–504.

Sharma, Y. R. (2007). *Elementary organic spectroscopy*. S. Chand Publishing.

Sharshira, E. M., & Hamada, N. M. M. (2012). Synthesis and antimicrobial evaluation of some pyrazole derivatives. *Molecules, 17*(5), 4962-4971.

Silva, V. L., Elguero, J., & Silva, A. M. (2018). Current progress on antioxidants incorporating the pyrazole core. *European Journal of Medicinal Chemistry, 156*, 394–429.

Silverstein, R. M., Webster, F. X., & Kiemle, D. J. (2014). *Spectrometric identification of organic compounds.* Wiley.

Verma, C., Thakur, A., Ganjoo, R., Sharma, S., Assad, H., Kumar, A., & Alfantazi, A. (2023). Coordination bonding and corrosion inhibition potential of nitrogen-rich heterocycles: Azoles and triazines as specific examples. *Coordination Chemistry Reviews, 488*, 215177.

Zhang, J., Xu, L., & Wong, W. Y. (2018). Energy materials based on metal Schiff base complexes. *Coordination Chemistry Reviews, 355*, 180–198.